

Steering through Successive Objects

Shota Yamanaka
Yahoo Japan Corporation
Chiyoda, Tokyo, Japan
syamanak@yahoo-corp.jp

Wolfgang Stuerzlinger
Simon Fraser University
Vancouver, Canada
w.s@sfu.ca

Homei Miyashita
Meiji University
Nakano, Tokyo, Japan
homei@homei.com

ABSTRACT

We investigate stroking motions through successive objects with styli. There are several promising models for stroking motions, such as crossing tasks, which require endpoint accuracy of a stroke, or steering tasks, which require continuous accuracy throughout the trajectory. However, a task requiring users to repeatedly steer through constrained path segments has never been studied, although such operations are needed in GUIs, e.g., for selecting icons or objects on illustration software through lassoing. We empirically confirmed that the interval, trajectory width, and obstacle size significantly affect the movement speed. Existing models can not accurately predict user performance in such tasks. We found several unexpected results such as that steering through denser objects sometimes required less times than expected. Speed profile analysis showed the reasons behind such behaviors, such as participants' anticipation strategies. We also discuss the applicability of exiting performance models and revisions.

Author Keywords

Graphical user interfaces; human motor performance; steering; crossing; pen computing.

ACM Classification Keywords

H.5.2. [Information interfaces and presentation]: User Interfaces – Theory and methods.

INTRODUCTION

Studying models of human motor performance is a core topic in the human-computer interaction (HCI) field. In addition to deriving new models, testing the validity of existing models in different circumstances is also important. As a well-known example, Fitts' law [18] has been confirmed to hold for various kinds of tasks [46]. Besides, creating appropriate models for a given task condition is also important for modeling task performance. For example, when a pointing task is extremely easy (Fitts' index of difficulty is less than 3 bits), solely the movement distance affects the performance [20, 22]. Thus, knowledge of the limits of existing models

gives us a better understanding when a given model is appropriate.

We investigate the performance of stroking motions in a situation as shown in Figure 1a; where users make a stroke while avoiding obstacles. Such motions are required for lassoing objects in illustration or presentation software. Here, we focus on straight stroking motions, as illustrated in Figure 1b-f, which form a crucial step towards a better understanding of general lassoing motions.

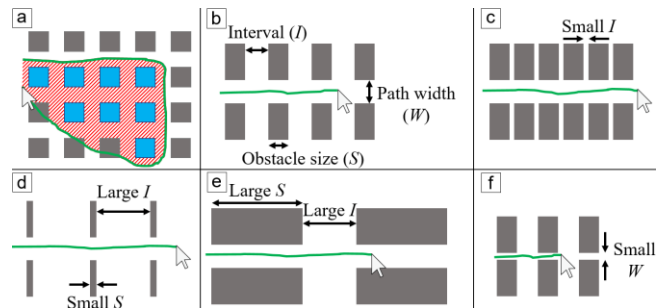


Figure 1. (a) Lassoing icons. Icons whose entire area is inside of the loop are selected (highlighted in blue). The start and end points are automatically closed. The work presented here focuses on the straight stroking segments. (b-f) Steering through obstacles with various conditions.

Here we investigate which predictive model is suitable to forecast user performance for such straight stroking motions. Based on previous work, three parameters are likely to affect user performance, as illustrated in Figure 1b. If the inter-obstacle distances in the direction of the movement (here interval I) are very small (Figure 1c), this task could be modeled by the steering law [1]. Instead, if intervals are large and the obstacle size (S) small (Figure 1d), this could be regarded as a series of crossing tasks [1, 4]. Else, for large intervals and passing through obstacles with large S (Figure 1e), the task could be modeled partially by the steering law, while entering each successive pair of obstacles could be modeled by the crossing law [55]. Lastly, as predicted by both the steering and the crossing laws, the width (W) of the path should affect movement time; as W decreases, speed decreases (Figure 1f). Although lassoing performance has been studied [9, 25], we found no work that distinguishes between the above-mentioned models for a common range of task conditions.

To better understand the stroking motions, and for selecting appropriate models for each task, we conducted an experiment to investigate the effects of task parameters of

Permission to make digital or hard copies of all or part of this work for personal or classroom use is granted without fee provided that copies are not made or distributed for profit or commercial advantage and that copies bear this notice and the full citation on the first page. Copyrights for components of this work owned by others than the author(s) must be honored. Abstracting with credit is permitted. To copy otherwise, or republish, to post on servers or to redistribute to lists, requires prior specific permission and/or a fee. Request permissions from Permissions@acm.org.
CHI 2018, April 21–26, 2018, Montreal, QC, Canada

© 2018 Copyright is held by the owner/author(s).

Publication rights licensed to ACM.

ACM 978-1-4503-5620-6/18/04...\$15.00

<https://doi.org/10.1145/3173574.3174177>

obstacle interval (I), tolerance width of the path trajectory (W), and obstacle size (S). Our contributions include:

- 1) We validate prediction accuracies of existing models: the crossing law, steering law, and a ballistic model combining the two laws. Results show that the ballistic model is not necessary, but also that a combination of the crossing and steering laws show the best prediction scores both in R^2 and AIC values.
- 2) Based on a speed profile analysis, we discuss the effects of I , W , and S . We identify that participants anticipate future obstacles and adapt their speed depending on the subsequent path width. They tend to move slower than the speed associated with the future path, even when the pen-tip is currently within one of the interval segments.
- 3) We also analyze if participants perform open- or closed-loop motions and found evidence for both as well as combinations. For example, users performed a series of crossing motions for the longest intervals (152 mm), a single steering motion for the shortest ones (2 mm), and a combination for medium intervals (42 and 92 mm).

RELATED WORK

In this section and afterwards, a and b in equations are empirically determined regression coefficients.

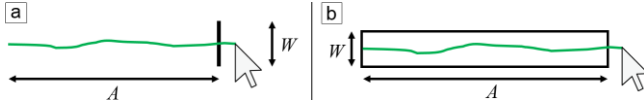


Figure 2. (a) A crossing law task and (b) a steering law task.

Crossing Law

The crossing law [4] shows that the movement time (MT) to cross a goal line of length W at a distance A from the initial position (see Figure 2a) is modeled by Fitts' law [18, 31]:

$$MT = a + b \log_2 \left(\frac{A}{W} + 1 \right) \quad (1)$$

where the logarithmic term is called index of difficulty of crossing tasks (ID_C):

$$ID_C = \log_2 \left(\frac{A}{W} + 1 \right) \quad (2)$$

This relationship has been confirmed to hold for various input devices [19, 29, 50]. Crossing outperforms pointing in certain conditions for stylus operations [7, 41, 50]. For a condition with large interval (I) and small obstacle size (S), we assume that the crossing law models the movement through such a tunnel well. More effective techniques and tools have been proposed [6, 8, 30, 38, 47, 56]. Conditions for crossing motions have been also studied, such as crossing angles [7] and land-on/take-off distances [14].

For pointing tasks, when the target width (W) is too large, users do not have to carefully position the cursor on the target. Thus, MT tends to be affected only by A [20]:

$$MT = a + b\sqrt{A} \quad (3)$$

We assume that this model for pointing tasks can also be applied for crossing tasks with large W . This assumption is not new [21], yet has not been tested empirically.

Laws of Steering

Steering Law

Models of steering motions have been proposed for several purposes [16, 39, 40]. In the HCI field, Accot and Zhai's global form of the steering law [1] is a well-known model:

$$MT = a + b \int_C \frac{dx}{W(x)} \quad (4)$$

where C is a given path, x is a position in the path, and $W(x)$ is the path width at x . For a linear and constant-width path as shown in Figure 2b, the model simplifies to:

$$MT = a + b \frac{A}{W} \quad (5)$$

where A is the path length and W is the path width. A/W is called the index of difficulty for steering tasks (ID_S):

$$ID_S = \frac{A}{W} \quad (6)$$

Another formulation of the steering law is:

$$V = a + bW \quad (7)$$

where V is the average speed for the entire path: $V=A/MT$. Although Equation 7 tends to show a relatively worse model fit than the MT form (Equation 5) [21], they both imply that speed increases linearly with path width. Some researchers recommend to use the *effective width method* for both Fitts' [31, 46] and steering [23] laws. Yet, we use only nominal parameter values here due to concerns raised in previous work, e.g., Zhai [57] and Wright and Lee [51]. The steering law holds for many computer input devices [2], changes of motor scale [3], movement angle [49], temporal constraint [61], speed- or accuracy-emphasized conditions [62], car driving [59], narrowing and widening path shapes [53, 54], and implicit path tolerance (a condition where the path boundary is not visible) [23].

While Equation 7 uses the speed in the entire path, Accot and Zhai also proposed an instantaneous speed model [1] that is proportional to the current path width:

$$v(x) = \frac{W(x)}{\tau} \quad (8)$$

where $v(x)$ is the speed at the position x , and τ is the empirically-determined time constant.

Other Variations for Steering Operations

Although the steering law models, Equations 5 and 7, have been validated in various tasks, refined versions are required for some conditions. For example, models for steering through a path with a corner [37] and pointing at a target after steering a path [24, 44] have been proposed.

When the path width W is too large, users can ignore the path boundary, and thus W does not affect the movement speed and the operational time [1, 7, 16, 17, 27, 44, 45, 48, 49]. In such conditions, V is limited by the user’s motor performance, and MT is affected only by the path length A [48]. The steering model then takes the same form as the ballistic Fitts’ law model (Equation 3). This model is appropriate for large W conditions in our work.

While the above models target a single path segment, recent work investigated steering through sequential path segments [55]. In their study, participants had to steer through two straight, connected path segments. Although a model derived from the global one (Equation 4) fit well, participants significantly changed their strategy contingent on the path narrowing or widening. Moreover, it is hard to predict if we can directly apply Yamanaka et al.’s [55] findings to more general tasks, such as the tasks illustrated in Figure 1, i.e., if the global steering model can be used for sequential path segments. As our work includes many more path segments (up to 62 obstacles), the empirical results will deepen our understanding of steering actions.

Lassoing Operations

To facilitate the selection of larger groups of objects, several researchers have presented group selection methods [12, 13, 26, 28, 35, 43, 47, 52], which include various lasso and/or brush-based selection techniques. A first, high-level model of group selection [9] proposes a linear model for time and task difficulty.

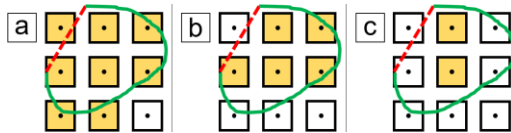


Figure 3. Potential criteria to detect which objects are lassoed. Yellow-highlighted icons are selected by the green stroke. The loop between start and end points is automatically closed, as depicted by the red dotted lines. (a) Objects inside of a loop or crossed by the stroke, (b) objects whose center is inside of the loop, and (c) objects whose entire area is inside of the loop. The work presented here directly applies to the last criterion.

There are several ways to decide how objects are selected by a lassoing operation. For example, in Adobe Illustrator CS6, objects inside of an enclosed loop or objects crossed by the stroke are selected (Figure 3a). Mizobuchi and Yasumura [34] proposed that objects whose center point is inside of an enclosed loop are selected (Figure 3b). The scope of our experiments matches a widely-used criterion, namely that only objects inside the lasso loop that are not touched by a stroke are selected, as in, e.g., Apple Keynote (Figure 3c). This is equivalent to having the user avoid touching obstacles as shown in Figure 1. Note that the different lasso criteria shown in Figure 3 permit the user to effectively draw through a wider tunnel compared to the task portrayed by the object spacing. Given that this could confuse users, we remove this confound here, by matching the visual appearance of the tunnel to the task requirements.

In summary, existing models can accurately predicts user performance for passing through a single goal line [4], a single [1] or two path segments [37, 55] for both of ballistic and visually-controlled movements. Also, the number of icons can predict lassoing time [9]. Yet, we wanted to explore if (a) steering performance through more than two goal/path segments is predicted by existing models, and (b) which task parameters affect user strategies and behaviors. Answers to these questions will lead to better understanding of more complex actions, such as lassoing multiple icons.

RESEARCH QUESTIONS

Appropriate Models and Parameter Interactions

The steering law was derived through the assumption that steering involves an infinite number of crossing motions [1, 59]. Yet, no one empirically confirmed if the steering law applies to a *limited* number of crossing motions. E.g., when there are 51 goals within 50 mm amplitude, i.e., goals at 1 mm intervals, as shown in Figure 4a (top), we assume that these 50 crossing tasks can be modeled by a single steering ID_S value. Yet, one can hypothesize that, as the number of goals decreases, the crossing law would become the more appropriate model, as shown in Figure 4a (middle, bottom).

Similar arguments can be made for another task parameter, the obstacle size S . While crossing law experiments used a 1-pixel (practically <1 mm) line as a target [1, 4, 7, 29, 30], does the crossing model hold for goals with a larger “thickness”, e.g., 5 or 20 mm, as shown in Figure 4b? The steering law holds for tasks that require continuous visual feedback; when $ID_S (=A/W)$ is greater than 8 [49] or 15 [45] bits. Otherwise, users can accomplish the task with only a ballistic movement [48]. However, these thresholds were confirmed only for tasks with single path segments.

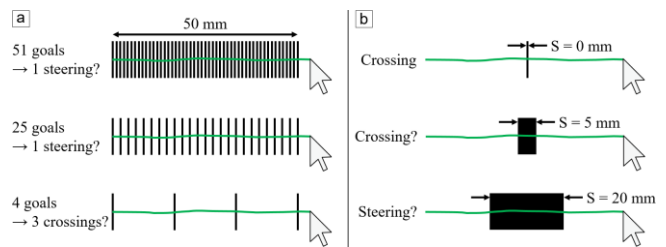


Figure 4. (a) The steering law is the appropriate model for short crossing intervals, but with larger intervals, multiple crossing laws could be more appropriate. (b) The crossing law would be appropriate for a short-distance goal line, but as the size increases, the steering law could become more appropriate.

Our central research question thus is: *which of the crossing or steering law (including models for ballistic movements) is more appropriate to predict such movements*, depending on given task conditions. Based on the above discussions, interval (I) and obstacle size (S) would transition user behavior between a crossing and a steering “mode” and back. Because the speed is limited by the trajectory width, W would affect performance as well. For example, when W is too large, we may not have to distinguish between crossing or steering, because they become the same model, equation 3.

When W is small, users steer the path more carefully and hence use a steering mode, even in shorter path amplitudes (S in Figure 4b) [48]. Thus, we aim to identify the interactions of I , W , and S in our work.

Single Steering versus Successive Crossing

When users move a stylus or a cursor from a wide path to a narrow path, they decelerate well in advance of the path joint [55]. Therefore, we assume that when faced with successive narrow path constraints with short intervals, as shown in Figure 1f, users cannot accelerate in the intervals and hence the task is better modeled by the steering law using the narrower constraint (i.e., W in Figure 1f) rather than the crossing law. More specifically, as shown in Figure 5, although wider path segments (W_1) might exist, users would adjust the speed in the narrower regions as predicted by the narrower width, W_2 . Hence, a potential model is:

$$MT = a + b \left(\frac{6(A_1 + A_2)}{W_2} \right) \quad (9)$$

rather than a model derived from the global steering law:

$$MT = a + b \left(\frac{6A_1}{W_1} + \frac{6A_2}{W_2} \right) \quad (10)$$

Such an assumption has been already proposed [15, 55]. We empirically test if such a condition can be modeled by Equation 9, i.e., we attempt to model this motion as a single steering task using the narrower width (W_2).

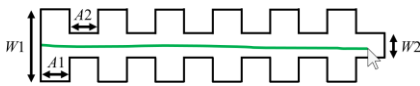


Figure 5. A sequence of six wide and six narrow alternating path segments.

PILOT STUDY

Before the main study, we conducted a pilot study to confirm our most fundamental hypothesis that the interval (I), obstacle size (S), and path tolerance width (W) parameters affect user performance.

Apparatus

The system was a Sony Vaio Z (Intel Core i7-5557U, 3.10 GHz, 4 cores; Intel Iris graphics 6100; 16 GB RAM; Windows 10 Pro). The input device and the display was a Wacom Cintiq 27 QHD Touch DTK-2700/K0 (27" diagonal, 596.7 × 335.6 mm active input area, 2560 × 1440 resolution, 4.29 pixels/mm; 12 ms response time). The experimental system was implemented with Hot Soup Processor 3.4 in full-screen mode. The system reads and processes input about 125 times per second. The pen tablet was positioned on a table in "stand" mode (20°, Figure 6a). All participants wore a cotton artist glove to reduce friction. They were informed that their palms could touch the surface, as we had disabled touch sensing.

Participants

Five volunteers participated in the experiment, two were female and three male. The average age was 23.4 years ($SD =$

2.06). All participants had normal or corrected-to-normal vision and were right-handed.

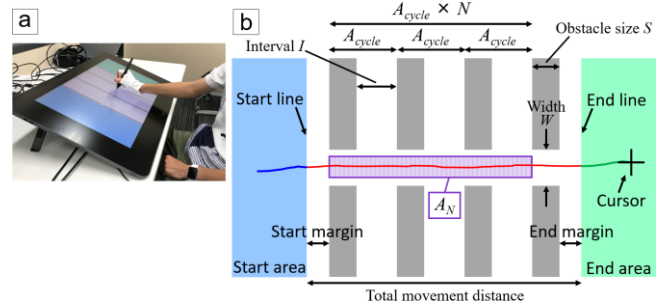


Figure 6. (a) Experimental setup and (b) visual stimuli. Our work focuses on the part of the stroke highlighted in purpose, which has length A_N . This corresponds to a cyclic movement criterion, see the text.

Task

We reused the color scheme from previous work [23, 53, 55] for the task areas: a blue starting area, a white path, and a green end area. Participants sat centered in front of the pen tablet at a comfortable distance to move the stylus on the surface (up to ~500 mm). They were asked to make a stroke from the start to the goal area as quickly and accurately as possible. A crosshair cursor left a trace from the moment of pen contact until lift-off. A bell sound confirmed that the cursor had crossed the end line. Participants were only permitted to stroke through white-colored regions. A beep sounded when the cursor touched a gray-colored obstacle. Then the participant had to retry the same task again. Such a touch was counted as an erroneous attempt. Consistent with other steering law studies [3, 53, 55], lifting the pen tip in a trial was not considered an error, but the participant still had to redo the task. Re-starting within a path or hovering was not permitted.

Design and Procedure

The total movement distance from the start line to the end line was fixed to 300 mm (or 1287 pixels). We tested combinations of two I , two W , and two S values as shown in Table 1. The total number of combinations of the parameters was $2(I) \times 2(W) \times 2(S) = 8$. One block consisted of a random ordering of the 8 conditions. Participants first performed a single practice block, and then six blocks for data collection. Movement direction was always to the right. The recorded data for the actual tasks were 8 conditions × 6 blocks × 5 participants = 240 trials. Participants took 4 to 5 minutes from the instructions to the completion of all tasks.

	I	W	S
mm	2	92	8
pixel	8	394	34
			32
			137
			21
			343

Table 1. I , W , and S values tested in the pilot study.

Data Analysis

The margin from the start line to the first obstacle differed depending on the combination of I and S . Thus, we cannot use the movement time from the start to the end line as MT in

the existing models. In addition, because the crossing law assumes that the goal line has no thickness ($S = 0$), and the steering law ignores the time to enter a path segment, we cannot directly apply existing models to our experimental conditions. Based on this reasoning, we analyzed the obtained data with a *cyclic movement criterion*, as shown in Figure 6b. If there are $(N+1)$ obstacle pairs, participants repeatedly crossed or steered through obstacles N times. Hence, the movement amplitude for a single cycle, A_{cycle} , is $(I+S)$, and the amplitude for N cycles, A_N , is $(A_{cycle} \times N)$ or $((I+S) \times N)$. We define the time required for the distance of A_N as MT_N , and the time for a single cycle as $MT_{cycle} = MT_N/N$. Although other definitions are possible, e.g., A_{cycle} could be the distance between the centers of two successive obstacles, there would be only a small difference in terms of MT_N between each different definition, if participants repeatedly steered through $(N+1)$ successive obstacle pairs for a sufficiently long total movement distance.

Because MT_N depends on the total distance for the movement amplitude A_N , a direct comparison of MT_N values for different I and S conditions is not sensible to analyze parameters effects. Instead, we compare the movement speed *normalized* to a single obstacle, i.e., $V_{avg} = A_N/MT_N$, which is (mostly) independent from the total movement distance, as it depends only on the ratio of time and distance.

Results

We recorded 266 trials including four lifting-pen instances (1.5%). After excluding these four, we identified 22 errors among 262 data points (8.4%). Following previous work [1, 2, 3, 53, 54, 55], we analyzed only error-free trials via repeated-measures ANOVA with a Bonferroni post hoc test.

Figure 7 shows the average speed, $V_{avg} = A_N/MT_N$. We observed a main effect for W ($F_{1,4} = 53.954$, $p < .01$, $\eta_p^2 = 0.931$) and a significant interaction for $I \times S$ ($F_{1,4} = 7.829$, $p < .05$, $\eta_p^2 = 0.662$). We observed no other significant effects.

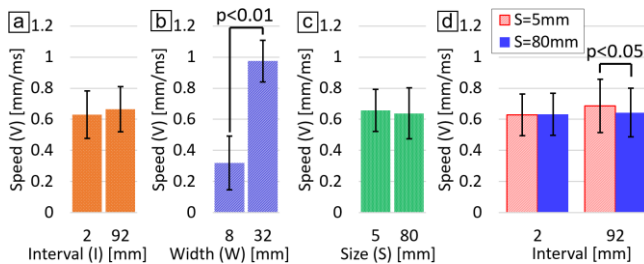


Figure 7. Results of the pilot study. Error bars show standard error.

Discussion of the Pilot Study

Although a limited number of trials were performed by only five participants, all parameters (I , W , and S) affected the average speed V as a main effect or an interaction, which indicates that we are indeed observing behavior changes.

Because both the crossing and steering laws predict that W affects MT (and thus V), it is not surprising that W has a main effect. We also observed the predicted interaction of $I \times S$.

When I is small (2 mm), the task resembles a single steering law task, as shown in Figure 1c. Thus, in this condition, V was not significantly affected by S , as shown in Figure 7d (the left pair of bars). On the other hand, when I was large (92 mm) and S was small (5 mm), the task resembles multiple crossing tasks (Figure 1d), and hence the speed was higher than in the steering conditions. When both I (92 mm) and S (80 mm) were large, the task resembles multiple steering tasks (Figure 1e), which reduces the speed compared to crossing. This significant difference is visible in the right pair of bars in Figure 7d.

Based on observations from our pilot study, participants seemed to move the stylus more slowly in steering motions, even for longer interval ($I = 92$ mm), rather than using successive crossing motions. Three of the participants did not perceivably accelerate in the intervals. This motivated us to include considerably larger I values in the main study. On the other hand, participants seemed to be unable to accelerate with shorter intervals ($I = 2$ mm) in each single steering motion; this is also shown in Figure 7d (left pair). Thus, we decided to evaluate intervals from 2 up to 152 mm.

For the wider tolerance ($W = 32$ mm), all participants rapidly steered the path regardless of the I and S values, as if they did not have to move the stylus carefully. For the narrower tolerance ($W = 8$ mm), all participants carefully steered the path, and sometimes made errors if their speed was a little too high. Hence, we can confirm that path width affected the performance. Therefore, we decided to re-use the range of 8 to 32 mm for W for the main study.

Based on our observation of participants' behaviors, $S = 5$ mm seemed to be a good approximation of a goal "line" in crossing tasks; for the longer intervals ($I = 92$ mm), two participants accelerated after passing through a pair of obstacles, and then decelerated to pass through the next pair, like a general crossing law task. On the other hand, $S = 80$ mm seemed to be still short, because two or three participants did not seem to exhibit steering behaviors between pairs of obstacles. This motivated us to include larger S values, e.g., 120 or 130 mm, in the main study.

MAIN STUDY

In this main study, we tested the effects of path parameter values on user performance more comprehensively. In addition to the pilot study metrics, we also collected data for more detailed analyses, such as plotting the speed profiles. Only the participants and path parameter values were changed from the pilot study.

Participants

Eleven volunteers participated, two were female, with an average age of 22.9 years ($SD = 2.61$). All participants had normal or corrected-to-normal vision and were right-handed. Three of them had also participated in the pilot study.

Design and Procedure

The total movement distance from the start to the end line was fixed to 420 mm (1801 pixels). The corresponding *land-*

on (in the start area) and *take-off* (in the end area) widths were sufficiently long (88 mm for each side). We tested four interval (I), three width (W), and four obstacle size (S) values, as shown in Table 2. One *block* consisted of a random ordering of $4(I) \times 3(W) \times 4(S) = 48$ conditions. Participants performed ten trials randomly selected from these conditions for training, and then four blocks for data collection. Movement direction was always to the right. The recorded data were $48 \text{ conditions} \times 4 \text{ blocks} \times 11 \text{ participants} = 2112$ trials. Participants took 12 to 15 minutes for this study.

	I				W			S			
mm	2	42	92	152	8	16	32	5	25	65	125
pixel	8	18	394	652	34	68	137	21	107	278	536

Table 2. I , W , and S values tested in the main study.

Results

We recorded 2331 trials. 22 instances (0.94%) of pen lifting were observed and excluded. A total of 197 errors (8.5%), where participants touched an obstacle, were identified. We analyzed only error-free trials via repeated-measures ANOVA with a Bonferroni post hoc test.

Error rate

We found a main effect of W ($F_{2,20} = 12.577, p < 0.001, \eta_p^2 = 0.557$). Other main effects and interactions were not significant ($p > 0.05$). Therefore, based on the speed-accuracy tradeoff [58, 61, 62], the effects of I and S should be visible in the speed results.

Average Speed

For average speed, $V_{avg} = A_N / MT_N$, all parameters showed main effects: I ($F_{3,30} = 41.637, p < 0.001, \eta_p^2 = 0.806$), W ($F_{2,20} = 379.267, p < 0.001, \eta_p^2 = 0.974$), and S ($F_{3,30} = 693.287, p < 0.001, \eta_p^2 = 0.986$). All interactions ($I \times W, I \times S, W \times S$, and $I \times W \times S$) were significant, all with $p < 0.001$.

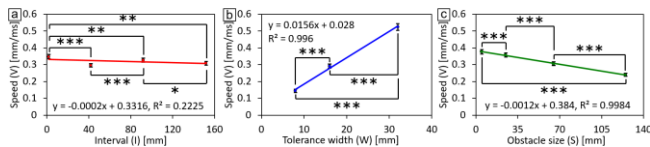


Figure 8. Results of the main effects. Error bars show standard error. (* $p < 0.05$, ** $p < 0.01$, *** $p < 0.001$)

Figure 8 illustrates the effects of the path parameters. We show regression lines for each one, even though some of the model fitness values are small. Figure 9 shows the interactions. Figure 9c and d show the same data, each with a different parameter shown on the x-axis (S versus I).

Discussion with Speed Profile Analysis

Figure 10a shows the speed profiles along the x-axis for all 48 conditions. Because the raw data at 8 ms sampling rate were very noisy, we re-sampled the cursor trajectories at 40 pixel intervals on the x-axis, which corresponds to 9.3 mm intervals. This re-sampling better reveals the difference in top and average speeds between crossing and steering motions, if users clearly exhibited the different behaviors.

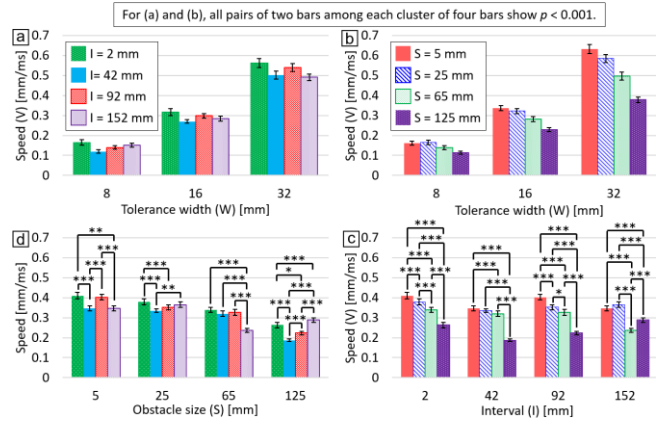


Figure 9. Results of the interactions. Error bars show standard error. (* $p < 0.05$, ** $p < 0.01$, *** $p < 0.001$)

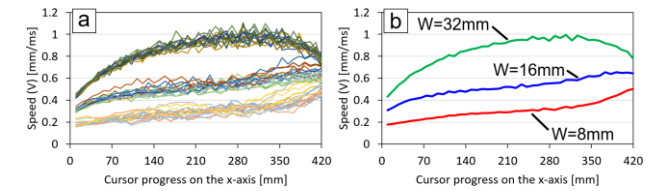


Figure 10. Speed profile for (a) all 48 conditions and (b) each W condition. Note that the speed at the start is not defined.

Effect of Path Width (W)

In Figure 10a, we can see three bands of speed “waves”, which seem to be separated by W values. Figure 10b shows the average speed profiles for each W value. Interestingly, while speeds for $W = 8$ and 16 mm gradually increased overall, the speed for $W = 32$ mm decreases from about ~ 330 mm onwards. Participants could perform arc-like movements in ballistic mode in this condition, and reached a top speed somewhere in the middle of the movement (roughly centrally in front of their body). Yet, they could not keep such a high speed until the end. In contrast, for the visually-controlled modes with $W = 8$ and 16 mm, they could keep accelerating until the end, which is consistent with steering law tasks in a single path segment [55]. Because operations modeled by Fitts’ law show short acceleration and long corrective movements [33], we regard movements in $W = 8$ and 16 mm as steering motions rather than crossing ones (disregarding the effect I and S values).

Effect of Interval (I)

Steering or Crossing Motions: To deeper analyze the speed profile, and to understand the obstacle parameter effects on participants’ strategies, we show several graphs that illustrate the behavioral differences. Figure 11 shows speed profiles for $W = 8$ mm (most visually-controlled condition) and $S = 5$ mm (thinnest obstacle condition).

As I decreases, we expected that the task to become more of a steering law task rather than crossing. Figure 11a ($I = 2$ mm) shows a typical steering motion with gradual acceleration, which is similar to the speed profiles reported in previous work (Figure 9 in [55]). On the other hand, Figure 11d ($I = 152$ mm) shows clear peaks in each interval;

participants began to accelerate after passing a pair of obstacles, and then decelerated to enter the next obstacle pair. Hence, we can empirically observe that participants performed a series of two crossing motions. In Figure 11c ($I = 92$ mm), we can see weak accelerations and decelerations in the intervals, but they are not as clear as in Figure 11d ($I = 152$ mm). We cannot find a clear peak in Figure 11b ($I = 42$ mm). Therefore, we see evidence that the transition between steering and crossing happens between $I = 42$ and 92 mm. These results show that, as expected, as I increased it changes participants' behaviors from steering to crossing.

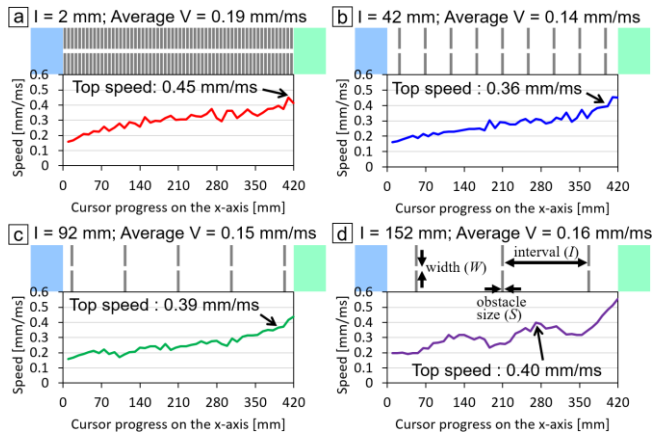


Figure 11. Speed profile for $W = 8$ mm and $S = 5$ mm. While speeds generally increase, for $I = 152$ mm there is clear evidence of several distinct crossing motions. While these speed profiles show the re-sampled instantaneous speed, average speeds are calculated by A_N/MT_N using the mean-of-means method for ANOVA. Thus, average speeds tend to be lower than the plotted speeds. Note: as we focus on N -cycle movements we ignore the speed after the final obstacle pair.

Top Speed and Average Speed: We expected that participants would attain higher speeds for larger values of I , because there were less obstacles to avoid. Interestingly, Figure 11 does not show such a clear increase in V_{avg} with increasing I . A potential reason is the point where we measure the top speed: the highest peak before the final obstacle. Because users gradually accelerate in a steering motion [55], the final peak could show the highest speed. Yet, Figure 11a and b show that the speed for $I = 2$ mm was usually higher than that for $I = 42$ mm throughout the path from start to end. Thus, the location for measuring the top speed cannot be the only factor.

Another potential explanation is that participants anticipate the next pair of obstacles. For $I = 2$ mm, they had to continuously attend to their pen-tip movement to avoid hitting the path boundary. Thus, they could only gradually reach the top speed, limited by the path width [48]. On the other hand, if obstacles were sparser, they had to avoid “hitting” the next obstacle when the pen-tip was within intervals. Because users tend to decelerate more than necessary before entering a path which is narrower than the current width tolerance [55], we assume that “new” decelerations were produced successively in such trials and

this affected the speed negatively. Thus, participants were not able to accelerate sufficiently in intervals, although the interval had practically infinite tolerance ($W = \infty$). In summary, and in contrast to our expectations, we identified that long intervals did not always increase the speed; the negative effect of decelerations might be greater than the positive effect of accelerations in intervals.

Figure 11 partially supports findings by Thibbotuwawa et al.’s steering tasks [48] as participants determine the current operational mode (open- or closed-loop) depending on the path width at about $5W$ in front of the current position. Because W in Figure 11 is 8 mm, the critical distance of anticipation would be 40 mm; if $I < 40$ mm, participants had to continuously anticipate the following obstacles and thus could not accelerate in intervals; if $I \geq 40$ mm, they could accelerate in intervals. While Figure 11b (I is 42 mm = $5.25W$) does not clearly show peaks in intervals, we believe that the “ $5W$ ” criterion is approximate. Moreover, Thibbotuwawa et al. [48] validated their “ $5W$ ” criterion with optical mice; direct input pen tablet could have a different critical distance of anticipation.

Effect of Obstacle Size (S)

We expected that participants would perform a steering motion for long S conditions and a crossing motion for short S conditions. This assumption can be analyzed for conditions with long I , because participants tended to perform a steering motion when I was short (Figure 11).

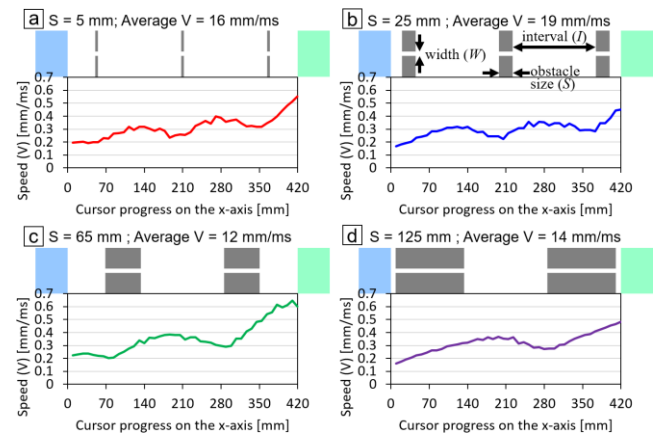


Figure 12. Speed profile in $I = 152$ mm and $W = 8$ mm.

Figure 12 shows the effects of S for $I = 152$ mm and $W = 8$ mm. Along with Figure 11d, all S conditions show clear acceleration and deceleration in the long intervals. Looking at the speed between a pair of obstacles, we can see a typical steering motion with gradual acceleration for the longest S (125 mm, Figure 12d). Yet, Figure 12b and c also show accelerations between pairs of obstacles. Because participants accelerated between a pair of obstacles and then kept accelerating inside the intervals (shown in Figure 12d), we cannot identify whether participants performed a steering or crossing motion for a midrange S value (25 and 65 mm, Figure 12b and c). Because the speed linearly decreased as S increased (Figure 8c), we assume that S has the effect of

forcing participants to perform more visually-controlled movements (steering rather than crossing). Yet, speed profiles from our experiment do not provide clear evidence of such behavior differences.

Model Fitting

Identifying which model is most suitable for predicting user performance in a single movement cycle is useful. Figure 13a and b shows the fits of the crossing (Equation 2) and steering law (Equation 6) for our data. Overall, the steering law shows a better fit than crossing. As both models include two degrees of freedom (a and b in equations), the difference cannot be due to model complexity.

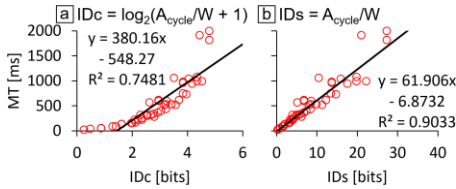


Figure 13. Model fitting for all the 48 data points.

To analyze the model fitness in more detail, we evaluate the effects of each of the task parameters. First, we analyzed when the ballistic model (Equation 3) is more appropriate. Figure 14 shows the fitness of the crossing, steering, and ballistic models in each row across different W values in the columns. The steering law is the best for all W values. Surprisingly, the ballistic model is not superior, even for the largest W (32 mm), although the speed profile showed that participants performed open-loop operations for $W = 32$ mm, as shown in Figure 10b. In this condition, the speed was not mainly constrained by the path width.

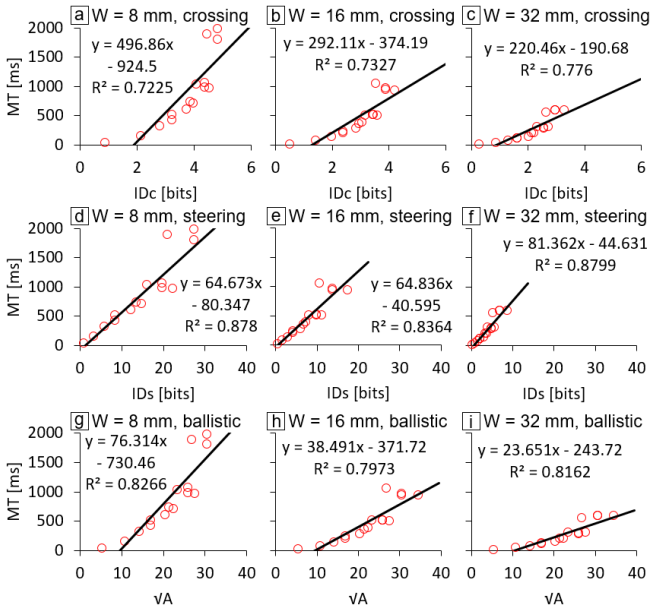


Figure 14. Model fitting for each W condition.

This result shows that using a model for ballistic operations for $W = 32$ mm is not appropriate, which supports related work on steering and Fitts' laws. For example, using

appropriate models for open- and closed-loop motions is preferred in terms of model fitness, e.g., using the ballistic model for $ID_S < 5$ bits in steering tasks [48], and for $ID < 3$ bits in pointing tasks [20]. However, the steering and Fitts' models also show reasonably high fitness without using the ballistic model, even when the task difficulty is low. Examples can be found in e.g., [2, 3] for steering and [32, 58] for pointing. Per our experimental results, it is not necessary to separate the models based on whether participants performed open- or closed loop motions.

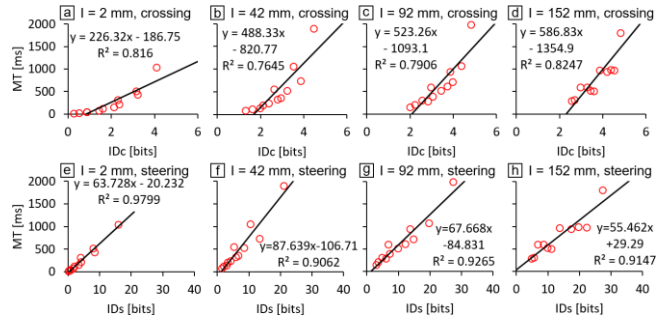


Figure 15. Effect of I on model fitting.

Second, we look at the effect of I on model fitness, because participants tended to perform crossing motions when intervals were longer (Figure 11). However, in contrast to our expectations, the crossing law shows a poorer fit than the steering law even for the longest I values, as shown in Figure 15d. The reason might be that these data include instances where participants performed steering motions when S was large (Figure 12).

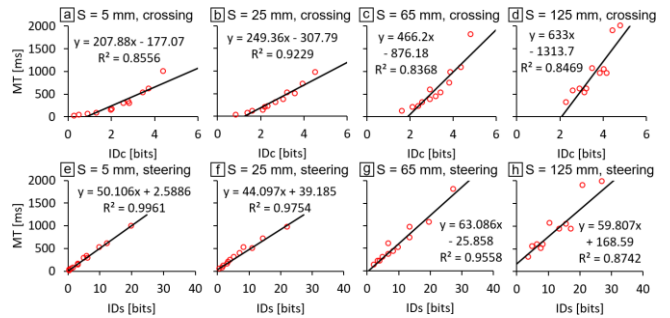


Figure 16. Effect of S on model fitting.

Third, our expectation that a longer S forced participants to perform steering motions rather than crossing ones is also rejected. As shown in Figure 16, overall the steering law shows a better fit than crossing. However, the steering law fitness tends to decrease as S increases, which still does not support our assumption.

In summary, we found that (1) the ballistic mode model shows poor fits and thus is not appropriate for prediction, (2) the steering law can usually model user performance better than the crossing law, and (3) the effects of I and S do not meet our expectations. In the general discussion section below, we derive and discuss a more appropriate model.

GENERAL DISCUSSION

Average Speed and Speed Profile

As expected, the average speed (V) increased as the path width (W) increased (Figure 8b), which is consistent with previous crossing and steering studies. In addition, as shown in Figure 8c, V decreased as the obstacle size (S) increased. This result supports previous work, which shows that more visually-controlled movements are required for longer paths in steering tasks [48]. We also evaluated whether V increased with the interval (I), because users were assumed to accelerate more in longer intervals. However, as shown in Figure 8a, we could not observe a clear tendency; the slope of the regression was nearly zero and R^2 was 0.22. Although I showed a significant main effect, we discuss potential reasons behind the lack of the interval's effect on V by analyzing the interactions below.

When I is small, we expected that the task is a steering task regardless of the S value (Figure 1c), as the motion requires continuous visual feedback. Thus, we assumed that S should have no significant effect on V when I is too small. Yet, interestingly, this hypothesis was rejected; the left-most cluster of four bars in Figure 9d shows that, while I was only 2 mm, all S pairs are significantly different. The other three clusters in Figure 9d also show, with exceptions, a similar tendency, i.e., that V decreases as S increases.

Figure 9c shows the same data as Figure 9d, but with the obstacle size S on the x-axis. We expected that V increases as I increases, but the fastest V values were observed for $I = 2$ mm when S was 5, 25, and 65 mm. Only when S was 125 mm, we finally observed the fastest V for the largest I value.

We expected that the effect of S decreases as W increases, because users would perform only ballistic movements. In other words, when $W = 32$ mm in Figure 9b, we expected that there would not be a significant difference. Yet, this hypothesis must be rejected. In addition, we had a similar assumption that I would have no effect when $W = 32$ mm, but this was also rejected (Figure 9a).

Some of our hypotheses were not supported. We believe that a potential reason is the path length. The local steering law posits that the instantaneous speed is proportional to the current path width (Equation 8). However, in steering tasks users gradually accelerate in a path [55], thus a path of longer amplitude should show a higher average speed, while a shorter path might not show the potential maximum speed [48]. As the obstacle density was different depending on the combination of I and S , the margins between the start line and the first obstacle were also different. In our experiment, when the start and end margins were long, A_N became short, and thus the effect of a larger I value, which increased the V value, could be cancelled. As the obstacles could not “fill up” the total movement distance in some cases, depending on I and S values, A_N tended to be short.

Another explanation would be that participants anticipated subsequent movements [53, 54, 55]; in other words, they performed motor planning between 150 and 200 ms before

they reached the target [36]. When I is small, the task is a steering task, thus users could only gradually accelerate during the entire movement. On the other hand, when there are path joints, users significantly decelerate in advance of them [55]. We assume that in our experiment such decelerations were repeatedly performed for steering through sequential obstacles.

Model Refinement

In the model fitting analyses, we applied the steering and crossing laws for a single movement cycle, which predicts the entire movement for the distance of A_N . We ideally would like to model the total movement time in a stroking motion, but steering and crossing models were created for specific motions. Hence, a singly cycle of movement, which involves both a constrained path (S area) and an unconstrained interval (I area), is challenging to model.

A more sensible way to model user performance would be that we regard each movement cycle as a steering motion followed by a crossing motion:

$$MT = a + b \left(\frac{S}{W} \right) + c \log_2 \left(\frac{I}{W} + 1 \right) \quad (11)$$

where a , b , and c are empirically determined constants. A benefit of this “combined steering and crossing” model (hereafter ID_{SC} model) is the balance between the degrees of difficulty for two kinds of motions.

Table 3 summarizes the model fitness for all 48 conditions' data points. Because the ID_{SC} model includes three regressions coefficients, while the crossing and steering laws include only two, we also show Akaike information criterion (AIC) values [5, 10] in addition to R^2 . AIC balances the complexity of the model, i.e., the number of free parameters, and the fitness, and determines the comparatively best model. A model with (a) lower AIC value is a better one, (b) $AIC \leq (\text{minimum-}AIC + 2)$ considers comparisons with better models, and (c) $AIC \geq (\text{minimum-}AIC + 10)$ is safely rejected. This analysis method has been used to evaluate performance models [11, 42, 55, 60]. Based on the obtained AIC values, we can state that the ID_{SC} model can more accurately capture user performance than the crossing and steering laws.

Model	a	b	c	R^2	AIC
ID_C	-548 [-755, -341]	380 [315, 446]		0.748	676
ID_S	-6.87 [-80.1, 66.4]	61.9 [55.9, 67.9]		0.903	631
ID_{SC}	-167 [-248, -85.9]	85.0 [75.3, 94.6]	190 [158, 221]	0.926	620

Table 3. Model fitness and AIC values for the considered models with estimated coefficients, including 95% CIs [lower, upper]. a , b , and c are regression coefficients in each model.

For the overall performance, we highlight that participants did not perform only a single steering or a series of crossing motions. Based on the speed profiles there seems to be no clear thresholds for path parameters that would force participants to perform a specific kind of motion (Figure 11

and 12), because users were in the ambiguous transition region between steering and crossing. In addition, because all three parameter types (I , W , and S) significantly interacted with each other, the ID_{SC} model cannot improve the prediction accuracy that much. Still, per the difference of AIC 's between the best and second-best model (ID_S): 11 (= 631 – 620), the improvement is statistically significant.

Implications

We identified that participants performed motions as predicted by the literature only in limited cases: crossing motions for large I (Figure 11d), and steering motions when I was small (Figure 11a and b) or when S was large (Figure 12d). We also found that the ballistic model could not accurately model user performance, although $W = 32$ mm seemed to require open-loop motions (Figure 10). Our results empirically support Drewes' hypothesis ([15], Figure 5); applying the narrower W to the entire motion is suitable, rather than using the global steering law. As shown in these instances, we confirmed that there are many conditions that existing models cannot model well. Thus, it is necessary to validate whether we could apply an existing model to a given task, e.g., if the speed of a lasso stroke is always limited by the narrowest tolerance width? If so, we should use the steering law with the narrowest width rather than a global steering law. From this standpoint, we obtained a better understanding as to which performance model is appropriate for a given task.

Based on our results, researchers and UI designers who want to develop or evaluate selection techniques, such as [9, 34], can use our work to design evaluation tasks. For example, we recommend 8–16 mm icon margins (I and S in our study) to compare user performance of selection techniques; with 32-mm margins, user speed would be determined by the upper limit of motor skills rather than task difficulty. Other implications include (a) adjusting task difficulty in video games, e.g., for steering a character through obstacles with varying distances and sizes, (2) choosing appropriate thresholds for lassoing operations, e.g., for the inclusion and exclusion of objects, in drawing/painting and other applications that involve lassoing and (3) accurately measuring steering skills when driving a real/virtual car through obstacles [39, 40, 59].

An application of our work that could improve GUI operations, is to visually fill empty space among objects as shown in Figure 17. Because a medium range of I values sometimes decreases the movement speed (Figure 11), we speculate that visually “removing” the intervals through showing visual hulls can improve user performance, as users do not need to decelerate to pass through the next pair of objects. Still, we recommend that such hulls serve only as visual guides. Then, users can still accomplish a lasso operation even if their stroke touches the red circumferences, as shown in the bottom-left of Figure 17b. As such effects visually straighten the path, users might also change their behavior to avoid touching the red boundary. Clustering objects automatically is challenging, and here we simply

chose three groups determined by their proximities depicted through rectangles for bounding hulls. Evaluating the efficacy of this idea is subject to future work.

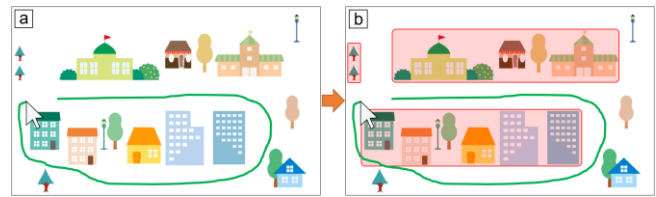


Figure 17. This proposed illustration software automatically shows visual guidelines to fill up empty spaces during lassoing operations, which we predict to lead to better performance.

Limitations and Future Work

We designed our experiment to observe the effects of I , W , and S independent of any specific model for wide ranges of task parameters. Still, we only tested regularly arranged obstacles, corresponding to a grid-like layout of icons/boxes. Yet, in GUI applications objects are sometimes irregularly arranged. Also, objects in illustration or presentations software often have non-uniform shapes, such as clouds or polygons. We may also test other devices (e.g., mice or touchscreens) operated by people with a wider range of motor abilities. Verifying the applicability of our current findings for such conditions requires further study.

To achieve our long-term goal, i.e., to derive a model for a complete lassoing movement in this work, we need to explore additional challenges. First, our cyclic movement criterion does not include the motion for “entering” the first obstacle. Also, lassoing icons involves making a curved stroke [25, 37], see Figure 1a, which cannot be modeled by our work. Furthermore, overall speed gradually increased throughout a trial as shown in Figure 11 and 12, but lassoing requires deceleration at corners. This makes modeling an entire lassoing movement more challenging.

CONCLUSION

In this study, we investigated straight stroke movements constrained by obstacles, which simulates a part of lassoing operations through icons. Participants' behaviors were significantly affected by the task parameters of interval (I), tolerance width (W), and obstacle size (S). Yet, the observations did not match all expectations. Although participants could accelerate more in longer intervals, the results show for longer intervals did not always show an increase in the stroke speed. Such unexpected behaviors have not been reported before, but are important for a better understanding of GUI operations, because the dependent variables (MT and V) could not be accurately modeled by existing work. Our proposed ID_{SC} model is simple, yet more accurate than previous work and forms a strong foundation for future models.

REFERENCES

1. Johnny Accot and Shumin Zhai. 1997. Beyond Fitts' law: models for trajectory-based HCI tasks. In *Proceedings of the SIGCHI Conference on Human Factors in Computing*

- Systems* (CHI '97), 295–302.
<http://dx.doi.org/10.1145/258549.258760>
2. Johnny Accot and Shumin Zhai. 1999. Performance evaluation of input devices in trajectory-based tasks: an application of the steering law. In *Proceedings of the SIGCHI Conference on Human Factors in Computing Systems* (CHI '99), 466–472.
<http://dx.doi.org/10.1145/302979.303133>
 3. Johnny Accot and Shumin Zhai. 2001. Scale effects in steering law tasks. In *Proceedings of the SIGCHI Conference on Human Factors in Computing Systems* (CHI '01), 1–8. <http://dx.doi.org/10.1145/365024.365027>
 4. Johnny Accot and Shumin Zhai. 2002. More than dotting the i's --- foundations for crossing-based interfaces. In *Proceedings of the SIGCHI Conference on Human Factors in Computing Systems* (CHI '02), 73–80.
<https://doi.org/10.1145/503376.503390>
 5. Hirotugu Akaike. 1974. A new look at the statistical model identification. *IEEE Transaction on Automatic Control*, Vol.19, No.6, 716–723.
<https://doi.org/10.1109/TAC.1974.1100705>
 6. Georg Apitz and François Guimbretière. 2004. CrossY: a crossing-based drawing application. In *Proceedings of the ACM Symposium on User Interface Software and Technology* (UIST '04), 3–12.
<https://doi.org/10.1145/1029632.1029635>
 7. Georg Apitz, François Guimbretière, and Shumin Zhai. 2010. Foundations for designing and evaluating user interfaces based on the crossing paradigm, *ACM Transactions on Computer-Human Interaction* (TOCHI), Vol.17, No.2, Article 9.
<https://doi.org/10.1145/1746259.1746263>
 8. Patrick Baudisch. 1998. Don't click, paint! Using toggle maps to manipulate sets of toggle switches. In *Proceedings of the ACM Symposium on User Interface Software and Technology* (UIST '98), 65–66.
<https://doi.org/10.1145/288392.288574>
 9. Per Bjerre, Allan Christensen, Andreas K. Pedersen, Simon A. Pedersen, Wolfgang Stuerzlinger, and Rasmus Stenholt. 2017. Predictive model for group selection performance on touch devices. In *Proceedings of the International Conference on Human-Computer Interaction* (HCI '17), 142–161.
https://doi.org/10.1007/978-3-319-58077-7_12
 10. Kenneth P. Burnham and David R. Anderson. 1998. Model selection and multimodel inference: a practical information-theoretic approach. Springer.
<http://dx.doi.org/10.1002/sim.769>
 11. Olivier Chapuis and Pierre Dragicevic. 2011. Effects of motor scale, visual scale, and quantization on small target acquisition difficulty. *ACM Transactions on Computer-Human Interaction* (TOCHI), Vol.18, No.3, Article 13.
<http://dx.doi.org/10.1145/1993060.1993063>
 12. Hoda Dehmeshki and Wolfgang Stuerzlinger. 2009. ICE-lasso: an enhanced form of lasso selection. In *Proceedings of IEEE Toronto International Conference of Science and Technology for Humanity* (TIC-STH '09), 630–635.
<https://doi.org/10.1109/TIC-STH.2009.5444424>
 13. Hoda Dehmeshki and Wolfgang Stuerzlinger. 2010. Design and evaluation of a perceptual-based object group selection technique. In *Proceedings of British Human Computer Interaction Conference* (BCS-HCI '10), 365–372.
 14. Morgan Dixon, François Guimbretière, and Nicholas Chen. 2008. Optimal parameters for efficient crossing-based dialog boxes. In *Proceedings of the SIGCHI Conference on Human Factors in Computing Systems* (CHI '08), 1623–1632.
<https://doi.org/10.1145/1357054.1357307>
 15. Heiko Drewes. 2013. A lecture on Fitts' law.
<http://www.cip.ifi.lmu.de/~drewes/science/fitts/A%20Lecture%20on%20Fitts%20Law.pdf>
 16. Colin G. Drury. 1971. Movements with lateral constraint. *Ergonomics*, Vol.14, No.2, 293–305.
<http://dx.doi.org/10.1080/00140137108931246>
 17. Colin G. Drury and E. B. Daniels. 1975. Performance limitations in laterally constrained movements. *Ergonomics*, Vol.18, No.4, 389–395.
<http://dx.doi.org/10.1080/00140137508931472>
 18. Paul M. Fitts. 1954. The information capacity of the human motor system in controlling the amplitude of movement. *Journal of Experimental Psychology*, Vol.47, No.6, 381–391.
<http://psycnet.apa.org/doi/10.1037/h0055392>
 19. Clifton Forlines and Ravin Balakrishnan. 2008. Evaluating tactile feedback and direct vs. indirect stylus input in pointing and crossing selection tasks. In *Proceedings of the SIGCHI Conference on Human Factors in Computing Systems* (CHI '08), 1563–1572.
<https://doi.org/10.1145/1357054.1357299>
 20. Khai-Chung Gan and Errol R. Hoffmann. 1988. Geometrical conditions for ballistic and visually controlled movements. *Ergonomics*, Vol.31, No.5, 829–839.
<https://dx.doi.org/10.1080/00140138808966724>
 21. Errol R. Hoffmann. 2009. Review of models for restricted-path movements. *International Journal of Industrial Ergonomics*, Vol.39, No.4, 578–589.
<http://dx.doi.org/10.1016/j.ergon.2008.02.007>
 22. Barry A. Kerr and Gary D. Langolf. 1977. Speed of aiming movements. *Quarterly Journal of Experimental Psychology*, Vol.29, No.3, 475–481.
<http://dx.doi.org/10.1080/14640747708400623>
 23. Sergey Kulikov, I. Scott MacKenzie, and Wolfgang Stuerzlinger. 2005. Measuring the effective parameters of

- steering motions. In *Extended Abstracts of the SIGCHI Conference on Human Factors in Computing Systems* (CHI '05), 1569–1572.
<http://dx.doi.org/10.1145/1056808.1056968>
24. Sergey Kulikov and Wolfgang Stuerzlinger. 2006. Targeted steering motions. In *Extended Abstracts of the SIGCHI Conference on Human Factors in Computing Systems* (CHI '06), 983–988.
<http://dx.doi.org/10.1145/1125451.1125640>
 25. Edward Lank and Eric Saund. 2005. Sloppy selection: Providing an accurate interpretation of imprecise selection gestures. *Computers & Graphics*, Vol.29, No.4, 490–500. <http://dx.doi.org/10.1016/j.cag.2005.05.003>
 26. Jakob Leitner and Michael Haller. 2011. Harpoon selection: efficient selections for ungrouped content on large pen-based surfaces. In *Proceedings of the ACM Symposium on User Interface Software and Technology* (UIST '11), 593–602.
<https://doi.org/10.1145/2047196.2047275>
 27. Jui-Feng Lin, Colin G. Drury, Victor Paquet. 2006. A quantitative methodology for assessment of wheelchair controllability. In *Proceedings of the Human Factors and Ergonomics Society Annual Meeting* (HFES '06), 1204–1207. <https://doi.org/10.1177/154193120605001119>
 28. David Lindlbauer, Michael Haller, Mark Hancock, Stacey D. Scott, and Wolfgang Stuerzlinger. 2013. Perceptual grouping: selection assistance for digital sketching. In *Proceedings of the International Conference on Interactive Tabletops & Surfaces* (ITS '13), 51–60.
<https://doi.org/10.1145/2512349.2512801>
 29. Yuexing Luo and Daniel Vogel. 2014. Crossing-based selection with direct touch input. In *Proceedings of the SIGCHI Conference on Human Factors in Computing Systems* (CHI '14), 2627–2636.
<https://doi.org/10.1145/2556288.2557397>
 30. Yuexing Luo and Daniel Vogel. 2015. Pin-and-cross: a unimanual multitouch technique combining static touches with crossing selection. In *Proceedings of the ACM Symposium on User Interface Software and Technology* (UIST '15), 323–332.
<https://doi.org/10.1145/2807442.2807444>
 31. I. Scott MacKenzie. 1992. Fitts' law as a research and design tool in human-computer interaction. *Human-Computer Interaction*, 91–139.
https://doi.org/10.1207/s15327051hci0701_3
 32. I. Scott MacKenzie. 2013. A note on the validity of the Shannon formulation for Fitts' index of difficulty. *Open Journal of Applied Sciences*, Vol.3, No.6, 360–368.
<http://dx.doi.org/10.4236/ojapps.2013.36046>
 33. David E. Meyer, Richard A. Abrams, Sylvan Kornblum, Charles E. Wright, and J. E. Keith Smith. 1988. Optimality in human motor performance: ideal control of rapid aimed movements. *Psychological Review*, Vol.95, No.3, 340–370.
<http://psycnet.apa.org/doi/10.1037/0033-295X.95.3.340>
 34. Sachi Mizobuchi and Michiaki Yasumura. 2004. Tapping vs. circling selections on pen-based devices: evidence for different performance-shaping factors. In *Proceedings of the SIGCHI Conference on Human Factors in Computing Systems* (CHI '04), 607–614.
<https://doi.org/10.1145/985692.985769>
 35. Thomas P. Moran, Patrick Chiu, and William van Melle. 1997. Pen-based interaction techniques for organizing material on an electronic whiteboard. In *Proceedings of the ACM Symposium on User Interface Software and Technology* (UIST '97), 45–54.
<https://doi.org/10.1145/263407.263508>
 36. Mathieu Nancel and Edward Lank. 2017. Modeling user performance on curved constrained paths. In *Proceedings of the SIGCHI Conference on Human Factors in Computing Systems* (CHI '17), 244–254.
<https://doi.org/10.1145/3025453.3025951>
 37. Robert L. Pastel. 2006. Measuring the difficulty of steering through corners. In *Proceedings of the SIGCHI Conference on Human Factors in Computing Systems* (CHI '06), 1087–1096.
<http://dx.doi.org/10.1145/1124772.1124934>
 38. Charles Perin, Pierre Dragicevic, and Jean-Daniel Fekete. 2015. Crosssets: manipulating multiple sliders by crossing. In *Proceedings of Graphics Interface* (GI '15), 233–240.
 39. Nicolas Rashevsky. 1959. Mathematical biophysics of automobile driving. *Bulletin of Mathematical Biophysics*, Vol.21, No.4, 375–385.
<http://dx.doi.org/10.1007/BF02477896>
 40. Nicolas Rashevsky. 1970. Mathematical biophysics of automobile driving IV. *Bulletin of Mathematical Biophysics*, Vol.32, No.1, 71–78.
<http://dx.doi.org/10.1007/BF02476794>
 41. Xiangshi Ren and Shinju Moriya. 2000. Improving selection performance on pen-based systems: a study of pen-based interaction for selection tasks. *ACM Transactions on Computer-Human Interaction* (TOCHI), Vol.7, No.3, 384–416.
<https://doi.org/10.1145/355324.355328>
 42. Xiangshi Ren, Jing Kong, and Xing-Qi Jiang. 2005. SH-model: a model based on both system and human effects for pointing task evaluation. *IPSJ Journal*, Vol.46, No.5, 1343–1353. <http://doi.org/10.2197/ipsjdc.1.193>
 43. Eric Saund, David Fleet, Daniel Larner, and James Mahoney. 2003. Perceptually-supported image editing of text and graphics. In *Proceedings of the ACM Symposium on User Interface Software and Technology* (UIST '03), 183–192. <https://doi.org/10.1145/964696.964717>
 44. Ransalu Senanayake, Errol R. Hoffmann, and Ravindra S. Goonetilleke. 2013. A model for combined targeting and

- tracking tasks in computer applications. *Experimental Brain Research*, Vol.231, No.3, 367–379.
<http://dx.doi.org/10.1007/s00221-013-3700-4>
45. Ransalu Senanayake and Ravindra S. Goonetilleke. 2016. Pointing device performance in steering tasks. *Perceptual and Motor Skills*, Vol.122, No.3, 886–910.
<http://dx.doi.org/10.1177/0031512516649717>
46. R. William Soukoreff and I. Scott MacKenzie. 2004. Towards a standard for pointing device evaluation, perspectives on 27 years of Fitts' law research in HCI. *International Journal of Human-Computer Studies*, Vol.61, No.6, 751–789.
<https://doi.org/10.1016/j.ijhcs.2004.09.001>
47. Sven Strothoff, Wolfgang Stuerzlinger, and Klaus Hinrichs. 2015. Pins 'n' touches: an interface for tagging and editing complex groups. In *Proceedings of the International Conference on Interactive Tabletops & Surfaces (ITS '15)*, 191–200.
<https://doi.org/10.1145/2817721.2817731>
48. Namal Thibbotuwawa, Errol R. Hoffmann, and Ravindra S. Goonetilleke. 2012a. Open-loop and feedback-controlled mouse cursor movements in linear paths. *Ergonomics*, Vol.55, No.4, 476–488.
<http://dx.doi.org/10.1080/00140139.2011.644587>
49. Namal Thibbotuwawa, Ravindra S. Goonetilleke, and Errol R. Hoffmann. 2012b. Constrained path tracking at varying angles in a mouse tracking task. *Human Factors*, Vol.54, No.1, 137–149.
<http://dx.doi.org/10.1177/0018720811424743>
50. Jacob O. Wobbrock and Krzysztof Z. Gajos. 2008. Goal crossing with mice and trackballs for people with motor impairments: performance, submovements, and design directions. *ACM Transactions on Accessible Computing (TACCESS)*, Vol.1, No.1, Article 4.
<https://doi.org/10.1145/1361203.1361207>
51. Charles E. Wright and Francis Lee. 2013. Issues related to HCI application of Fitts's law. *Human-Computer Interaction*, Vol.28, No.6, 548–578.
<http://dx.doi.org/10.1080/07370024.2013.803873>
52. Pengfei Xu, Hongbo Fu, Oscar Kin-Chung Au, and Chiew-Lan Tai. 2012. Lazy selection: a scribble-based tool for smart shape elements selection. *ACM Transactions on Graphics (TOG)*, Vol.31, No.6, Article 142. <https://doi.org/10.1145/2366145.2366161>
53. Shota Yamanaka and Homei Miyashita. 2016a. Modeling the steering time difference between narrowing and widening tunnels. In *Proceedings of the SIGCHI Conference on Human Factors in Computing Systems (CHI '16)*, 1846–1856.
<https://doi.org/10.1145/2858036.2858037>
54. Shota Yamanaka and Homei Miyashita. 2016b. Scale effects in the steering time difference between narrowing and widening linear tunnels. In *Proceedings of the Nordic Conference on Human-Computer Interaction (NordiCHI '16)*, Article 12.
<https://doi.org/10.1145/2971485.2971486>
55. Shota Yamanaka, Wolfgang Stuerzlinger, and Homei Miyashita. 2017. Steering through sequential linear path segments. In *Proceedings of the SIGCHI Conference on Human Factors in Computing Systems (CHI '17)*, 232–243. <https://doi.org/10.1145/3025453.3025625>
56. Chuang-Wen You, Yung-Huan Hsieh, Wen-Huang Cheng, and Yi-Hsuan Hsieh. 2014. AttachedShock: design of a crossing-based target selection technique on augmented reality devices and its implications. *International Journal of Human-Computer Studies*, Vol.72, No.7, 606–626.
<https://doi.org/10.1016/j.ijhcs.2014.03.001>
57. Shumin Zhai. 2004a. Characterizing computer input with Fitts' law parameters: the information and non-information aspects of pointing. *International Journal of Human-Computer Studies*, Vol.61, No.6, 791–809.
<https://doi.org/10.1016/j.ijhcs.2004.09.006>
58. Shumin Zhai, Jing Kong, and Xiangshi Ren. 2004b. Speed-accuracy tradeoff in Fitts' law tasks: on the equivalency of actual and nominal pointing precision. *International Journal of Human-Computer Studies*, Vol.61, No.6, 823–856.
<https://doi.org/10.1016/j.ijhcs.2004.09.007>
59. Shumin Zhai, Johnny Accot, and Rogier Woltjer. 2004c. Human action laws in electronic virtual worlds: an empirical study of path steering performance in VR. *Presence*, Vol.13, No.2, 113–127.
<http://dx.doi.org/10.1162/1054746041382393>
60. Jian Zhao, R. William Soukoreff, Xiangshi Ren, and Ravin Balakrishnan. 2014. A model of scrolling on touch-sensitive displays. *International Journal of Human-Computer Studies*, Vol.72, No.12, 805–821.
<https://doi.org/10.1016/j.ijhcs.2014.07.003>
61. Xiaolei Zhou, Xiang Cao, and Xiangshi Ren. 2009. Speed-accuracy tradeoff in trajectory-based tasks with temporal constraint. In *Proceedings of the IFIP International Conference on Human Computer Interaction (INTERACT '09)*, 906–919.
http://dx.doi.org/10.1007/978-3-642-03655-2_99
62. Xiaolei Zhou and Xiangshi Ren. 2010. An investigation of subjective operational biases in steering tasks evaluation. *Behaviour & Information Technology*, Vol.29, No.2, 126–135.
<http://dx.doi.org/10.1080/01449290701773701>